Instability and Dewetting of Confined Thin Liquid Films in Nonmiscible External Bulk Fluids (Water and Aqueous Surfactant Solutions): Experiments versus Theoretical Predictions

ARTICLE *in* LANGMUIR · JUNE 1998

Impact Factor: 4.46 · DOI: 10.1021/la9709756

3 AUTHORS, INCLUDING:

Dr. Hamidou Haidara
French National Centre for Scientific Research
85 PUBLICATIONS **469** CITATIONS
SEE PROFILE

Laurent Vonna
Université de Haute-Alsace
36 PUBLICATIONS **264** CITATIONS
SEE PROFILE

Research Article

Instability and Dewetting of Confined Thin Liquid Films in Nonmiscible External Bulk Fluids (Water and Aqueous Surfactant Solutions): Experiments versus Theoretical Predictions

Hamidou Haidara, Laurent Vonna, and Jacques Schultz

Langmuir, **1998**, 14 (12), 3425-3434 • DOI: 10.1021/la9709756

Instability and Dewetting of Confined Thin Liquid Films in Nonmiscible External Bulk Fluids (Water and Aqueous Surfactant Solutions): Experiments versus Theoretical Predictions

Hamidou Haidara,* Laurent Vonna, and Jacques Schultz

Institut de Chimie des Surfaces et Interfaces—ICSI-CNRS, 15 rue Jean Starcky, B.P. 2488, 68057 Mulhouse Cedex, France

Received August 28, 1997. In Final Form: March 2, 1998

We report new results of investigations on the dewetting of confined thin polydimethylsiloxane (PDMS) liquid films (~1 μm thick) from a nonwettable solid surface, in various immiscible external bulk liquids (pure water and aqueous surfactant solutions). The dewetting parameters of these systems, contact angles (θ_E, θ_D), and viscosity (η_{PDMS}, η_{EL}) are such that they both should belong to the theoretical regime where dewetting is expected to proceed as at a solid−PDMS−air interface, leading to a dewetting velocity V scaling as η_{PDMS}^{-1} (cf. to the subsection Position of the Problem and Previous Works). Our results do show some deviations from this, with velocities rather scaling as $\eta_{PDMS}^{-0.6}$ in surfactant solutions, while in pure water the η_{PDMS}^{-1} dependence is found after normalizing velocities with the logarithmic prefactor. In addition, the dewetting velocity in surfactant solutions is found to be 2 orders of magnitude higher than in pure water. These results are discussed from a fundamental standpoint, based on the strong alteration of both the magnitude and molecular weight dependence of the logarithmic prefactor (cutoff length, rim structure) as well as the emergence of additional terms which depend on the nature of the external liquid.

Introduction

Thin liquid films are commonly used or encountered in many industrial and technological applications, ranging from adhesives, paints, and textiles to lubricants and agrochemical. Aside these basic applications, there is a specific need to elaborate thinner films (approximately a few nanometers) for a wide range of applications such as electronics, TV screens, roll coatings, and optics. For these thin films, the coating speed and the nature of the fluid (complex fluid for instance) constitute the limiting factors to the process and stability of the coating. Therefore, it is important to understand how the dynamic stability of these films is affected by surfactants and particles entering the composition of complex fluids or by the confinement, as is the case for lubricant films or in automotive industries where oily steel substrates are directly coated by resins containing surface-active agents. In this latter case, one rather seeks for conditions where the thin oil film (approximately micrometer size) will rapidly dewet from the substrate and form nanosize droplets. These droplets can then be easily absorbed by the resin which will bind to the "dry" steel surface. In spite of these potential interests, much fewer investigations have been devoted to confined thin films involving complex media,[1−7] as compared to the important theoretical and experimental work[8−17] related to the stability and dewetting behavior of simple and polymeric liquid films at substrate−air interfaces.

In this paper, we address these problems of stability and dewetting of confined thin fluids through the case of thin liquid PDMS films, which dewet from a nonwettable hydrophobic substrate in pure water and surfactant solutions environments. The dewetting dynamics of these systems are studied as a function of the viscosity of the confined films and the nature of the boundary phases, and the results are compared to existing theoretical predictions which we first introduce in the following section.

Theoretical Background

Figure 1 depicts a thin liquid film dewetting from a nonwettable substrate in an air environment. Upon nucleation, a dry patch of radius R is formed which grows over time with a velocity $V = dR/dt$, while the liquid displaced from the patch is collected in the moving rim. In the limit of small dynamic contact angles ($\theta_D < 1$ rad) and assuming volume conservation, it has been shown that the dewetting velocity $V = dR/dt$ is independent of the film thickness and given by[2,10,13] $V = K_{DL} V^* \theta_E^3$, where $\theta_E = \theta_D\sqrt{2}$ is the contact angle at equilibrium of the liquid on the substrate. The constant $K_{DL} = (12 \ln(h/a)\sqrt{2})^{-1}$ depends on the logarithmic factor which involves the length h of the rim and the characteristic molecular size a of the dewetting liquid (DL). $V^* = (\gamma_L/\eta_L)$ represents a

* Corresponding author. E-mail address: H.Haidara@univ-mulhouse.fr.

(1) Joanny, J. F.; Andelman, D. *J. Colloid Interface Sci.* **1987**, *119*, 451.
(2) Brochard-Wyart, F. *J. Phys. II* **1994**, *4*, 1727.
(3) Brochard-Wyart, F.; de Gennes, P. G. *J. Phys.: Condens. Matter* **1994**, *6*, A9−A12.
(4) Brochard-Wyart, F.; de Gennes, P. G. *Langmuir* **1994**, *10*, 2440.
(5) Schull, K. R.; Karis, T. E. *Langmuir* **1994**, *10*, 334.
(6) Faldi, A.; Composto, R. J.; Winey, K. I. *Langmuir* **1995**, *11*, 4855.
(7) Basu, S.; Sharma, M. M. *J. Colloid Interface Sci.* **1996**, *1181*, 443.
(8) Srolovitz, D. J.; Safran, S. A. *J. Appl. Phys.* **1986**, *60* (1), 247.
(9) Haroon, S. K.; Scriven, L. E. *Chem. Eng. Sci.* **1991**, *46*, 519.
(10) Brochard-Wyart, F.; Martin, P.; Redon, C. *Langmuir* **1993**, *9*, 3682.
(11) Safran, S. A.; Klein, J. *J. Phys. II* **1993**, *3*, 749.
(12) Martin, J. I.; Wang, Z.-G. *Langmuir* **1996**, *12*, 4950.
(13) Redon, C.; Brochard-Wyart, F.; Rondelez, F. *Phys. Rev. Lett.* **1991**, *66*, 715.
(14) Reiter, G. *Langmuir* **1993**, *9*, 1344.
(15) Yerushalmi-Rozen, R.; Klein, J. *Langmuir* **1995**, *11*, 2806.
(16) Sheiko, S.; Lermann. E.; Möller, M. *Langmuir* **1996**, *12*, 4015.
(17) Stange, T. G.; Evans, D. F.; Hendrickson, W. A. *Langmuir* **1997**, *13*, 4459.

S0743-7463(97)00975-X CCC: $15.00
Published on Web 06/09/1998

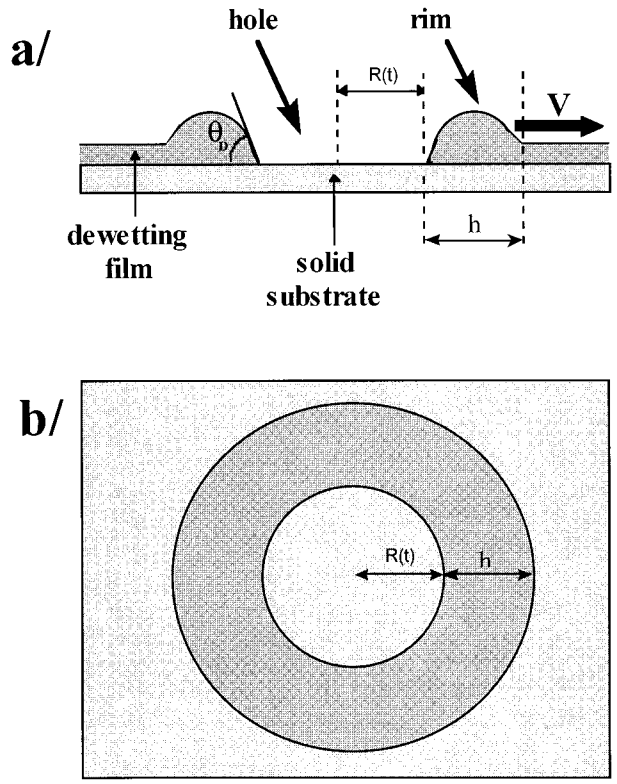

Figure 1. Sketch of a dewetting hole: (a) side view; (b) top view.

characteristic velocity depending exclusively on the nature of the liquid, its surface tension γ_L, and viscosity η_L. Theoretical predictions concerning these dewetting dynamics in air, especially the $(\eta_L)^{-1}$ dependence of V and the linear growth $R(t)$ of the dry patch, have been verified for metastable silicone oil and alkane films of different viscosities,[13] as well as for unstable polystyrene[14] films dewetting from various surfaces.

We now substitute the air environment of Figure 1 for a nonmiscible external fluid which may either be pure or complex and consider therefrom the stability and dewetting of that confined film. These problems have been theoretically discussed by Joanny and Andelman,[1] and later on by Brochard-Wyart and de Gennes.[2,4] It was shown from these theoretical works that so long as the dynamic contact angle satisfies the condition $\theta_D << 1 < (\eta_{DL}/\eta_{EL})$, the dissipation due to viscous frictions between the dewetting liquid and the external liquid can be totally neglected. The dewetting of such confined films should then be expected to proceed as if the external boundary liquid was replaced by air. These predictions result from the existence of different hydrodynamic regimes,[1,10] the solid-like and liquid behavior of the substrate, and the magnitude of the dewetting velocity. These hydrodynamic regimes are determined by two characteristic parameters: (i) the viscosity ratio (η_{DL}/η_{EL}) between the dewetting and external liquids, which has to be compared with the equilibrium contact angle θ_E, and (ii) the Reynolds number of the flow induced in the external liquid as the rim (of size h) moves, $R_e = (\rho_{EL}Vh/\eta_{EL})$. The relations between these parameters, especially that between (η_{DL}/η_{EL}) and θ_E, which determines the hydrodynamic regime and governs the dewetting dynamics of the confined film, are derived below, on the basis of the aforementioned theoretical works[10] and stressing the particular relevance to our experiments.

As the confined film dewets from the substrate, the liquid is collected in a rim which moves with a velocity V. The driving force for that motion is supplied by the unbalanced capillary force over the rim edges, which in the limit of small contact angles is given by[2,10]

$$F_D \cong \frac{1}{2}\gamma_{DL-EL}((\theta_E^2 - \theta_D^2) + \theta_D^2) = \frac{1}{2}\gamma_{DL-EL}\theta_E^2 \quad (1)$$

where we used the fact that $\theta_E = 0$ for the advancing (outer) edge of the rim which is in equilibrium with the native film.

For dewetting velocities corresponding to negligible Reynolds numbers of the flow in the external liquid, $R_e(EL) < 1$, the viscous dissipation over a region of size h in the external liquid has been derived by Joanny from scaling arguments as[10]

$$TS \sim \eta_{EL}\left(\frac{V}{h}\right)^2 h^2 = F_V V \quad (2a)$$

where the dissipative friction force per unit length of rim between the dewetting and the external liquids is obtained as

$$F_{V(DL/EL)} \sim \eta_{EL} V \quad (2b)$$

For higher dewetting velocities and Reynolds numbers, $R_e(EL) > 1$, one expects the crossover from the viscous to a viscoinertial regime, even for very low contact angles $\theta_D << 1 < (\eta_{DL}/\eta_{EL})$. In this viscoinertial regime and for a rim size h larger than $h_c = (\eta_{EL}^2/\rho_{EL}S)$, where S is the spreading parameter of the (solid−DL−EL) system, the flows in the external liquid are confined[10] in a diffusion layer of thickness d. In this regime, the friction force between the dewetting and the external liquids is given by[10]

$$F_{V(DL/EL)} = \eta_{EL}\left(\frac{h}{d}\right)V \quad (2c)$$

Irrespective of the dewetting regime (viscous or viscoinertial), the total viscous dissipation related to the motion of the confined rim always involves the basic contribution arising from the rim−solid substrate interface and given by (ref 10, p 3684)

$$F_{V(S/DL)} = 2\left(\frac{3\ln(h/a)}{\theta_D}\eta_{DL}\right)V \quad (2d)$$

In eq 2d, the local velocities of the advancing and receding sides of the rim V_A and V_R are assumed to be identical, leading to $(V_A + V_R) = 2V$.

The final balance between the capillary driving force (eq 1) and the different dissipative contributions at the liquid−liquid interface (eqs 2b and 2c) and solid−liquid interface (eq 2d) leads to the following expression for the dewetting velocity

$$V \propto \left(\frac{\gamma_{DL-EL}}{\alpha_{EL}\theta_E\eta_{EL} + \eta_{DL}\ln(h/a)}\right)\theta_E^3 \quad (3)$$

In eq 3, α_{EL} stands for the numerical factor in the viscous force $F_V = \alpha_{EL}\eta_{EL}V$, which for the viscoinertial regime (eq 2c) amounts to (h/d). In deriving eq 3, the dynamic contact angle θ_D appearing in relation 2d has been replaced by $\theta_E/\sqrt{2}$, still assuming the two wedges of the rim to move with the same velocity[10] V. In that case, equating the local velocities V_A and V_B corresponding respectively to the advancing and receding side of the rim, the relation $\theta_D = \theta_E/\sqrt{2}$ among the dewetting and equilibrium contact

angles is obtained (eqs 4a and 4b).

$$V_R \propto \frac{\gamma_{DL-EL}}{(\alpha_{EL}\theta_E\eta_{EL} + k_{DL}\eta_{DL})}\theta_D(\theta_E^2 - \theta_D^2) \qquad (4a)$$

$$V_A \propto \frac{\gamma_{DL-EL}}{(\alpha_{EL}\theta_E\eta_{EL} + k_{DL}\eta_{DL})}\theta_E^3 \qquad (4b)$$

The most related point which appears in eq 3 is the crossover between the two regimes of behavior of the boundary liquid phase, the "solid-like" and "liquid-like" behavior, which is determined by the relative magnitude of the viscosity ratio (η_{DL}/η_{EL}) and the contact angle θ_E in the denominator. For the dewetting dynamics of the confined film, which dissipative regime is dominant depends first on which boundary liquid-phase behavior is involved. This is characterized as mentioned above by the relative magnitude of (η_{DL}/η_{EL}) and θ_E. Inside these boundary substrate behaviors, velocity-dependent crossovers (viscoinertial, inertial) may be expected which are characterized by the Reynolds number R_e of the flows due to the rim motion.

In what follows, we will discuss our results along these different liquid1−liquid2 dewetting regimes, using for each (solid−DL−EL) system both reference data (ρ and η) and experimental values (θ_E, γ_{DL-EL}, and V).

The two substrate behaviors (regimes) characterized by the relative magnitude of θ_D and (η_{DL}/η_{EL}) are specified by the following boundary conditions[10]

$$\text{(i) } (\eta_{DL}/\eta_{EL}) < \theta_D < (\eta_{DL}/\eta_{EL})^{1/3}$$

$$\text{(ii) } \theta_D > (\eta_{DL}/\eta_{EL})^{1/3}$$

which hold and apply for dewetting contact angles $\theta_D = \theta_E/\sqrt{2} < 1$ rad $= 57°$. The maximum value observed for θ_D in our experiments was related to the dewetting in the aqueous surfactant solutions where $\theta_D = \theta_E/\sqrt{2} \sim 0.6$, for $\theta_E \sim 0.8$ as shown in Table 2. The inequality on the right hand side of the regime defined in condition i is then satisfied, since $\theta_D \sim 0.6 << (\eta_{DL}/\eta_{EL}) = (\eta_{PDMS}/\eta_{Water}) \sim 10^3$, making impossible the left hand side condition which requires that (η_{PDMS}/η_{WATER}) be $<\theta_D$. For about the same reason, the regime defined in condition ii is not relevant to these dewetting experiments, since the maximum value of θ_D (∼0.6) is negligibly small compared to (η_{PDMS}/η_{WATER})$^{1/3}$.

It then comes out that the basic assumptions prevailing for these two dewetting regimes just do not apply to any of our systems. The only theoretical liquid−liquid dewetting regime left[1,4] is that defined by the condition $1 < \theta_D < (\eta_{PDMS}/\eta_{WATER})$, which actually corresponds to the situation where the liquid film is expected to dewet as if the boundary liquid phase was replaced by air.[1,2,4] In that case, the predicted[1,4] dewetting velocity is

$$V = K_{DL}\left(\frac{\gamma_{DL-EL}}{\eta_{DL}}\right)\theta_E^3 \qquad (5)$$

where $K_{DL} = (12 \ln(h/a)\sqrt{2})^{-1}$.

On the basis of these theoretical works, one then expects our experiments characterized by contact angle values $\theta_E < 1$ and viscosity ratios (η_{PDMS}/η_{WATER}) on the order of 10^3 to belong to the dewetting regime $\theta_E < 1 << (\eta_{DL}/\eta_{EL})$ as defined above.

Before we discuss our results, we first present in the following section some of the previous experimental investigations related to the stability and dewetting dynamics of confined (solid−liquid1−liquid2) systems.

Previous Related Experimental Works

Experimental works dealing with the verification of predicted dewetting regimes for confined films are rather inexistent, especially for systems involving complex media. Among the sparse investigations, the paper by Shull and Karis[5] on the dewetting of thin films of poly(ethylene−propylene) (PEP) from poly(methyl methacrylate) (PMMA) and polystyrene (PS) substrates in various liquid alcohols represents to our knowledge, the most related work in this area. Though the high contact angles observed for these systems ($\theta_E \sim 180°$ for PEP drops on PMMA in liquid alcohol) still remain negligible as compared to (η_{DL}/η_{EL}), they are by far higher than 1 and do not satisfy the condition required for the regime $\theta_E < 1 << (\eta_{DL}/\eta_{EL})$ defined above to apply. When plotting their dewetting data as reduced velocities (V/γ) versus η_{PEP}, where γ is the changing PEP/boundary liquid interfacial tension which depends on the liquid alcohol, a scaling exponent for η_{PEP} close to -2 (~ -1.83) is obtained. In addition to this work (ref 5), few other investigations[6,7] mainly involve, as in ref 5, pure liquid phases, and rather most deal with the nucleation processes and morphology of the dewetting film. Finally, in spite of its theoretical and technological importance, dewetting in confined (solid−liquid1−liquid2) systems, either involving pure or complex liquids, has so far received much less attention, as compared to that in (solid−liquid−air) systems. The aim of this work is to contribute to fill this gap.

Experimental Section

The experimental procedure related to the creation of in situ wetting films has been presented in detail in a recent paper[18] which was mainly concerned with Marangoni flows in a (solid−liquid1−liquid2) system. Basically, the principle of the experiment consists in creating a Marangoni flow induced by the chemical gradient applied to a liquid drop, initially at rest on a solid substrate which is immersed in a nonmiscible external liquid. The liquid drops are silicone oils (PDMS) of different viscosity (from ABCR Karlsruhe, Germany), and the external liquids deionized and twice-distilled water. The solid substrate is a hexadecyltrichlorosilane (HTS)-treated Si wafer to give a hydrophobic methyl-terminated surface. The advancing and receding contact angles of these HTS surfaces against hexadecane and water in air are respectively $\theta_A \sim \theta_R \sim 42° \pm 1$ and $\theta_A = 110°$ and $\theta_R = 100°$ versus water. The surface tension gradient is created by placing on the solid surface, close to one edge of the drop (∼1 cm), about 10 μL of a concentrated aqueous surfactant solution (30 times the critical micelle concentration, cmc). The surfactant used in these experiments is a trisiloxane−ethylene oxide compound, $Me_3SiO[Me_2SiO-(EO)_8]SiMe_3$, which was kindly supplied from OSI-France (where its trade name is SILWET L-77). The surfactant is then transported upon deposition up to the triple line, where it adsorbs at the solid−liquid PDMS drop−external liquid interfaces, creating a strong Marangoni motion over the droplet which flows toward the virgin side. Because the triple line of the drop stays pinned a while on both sides, the first step of the Marangoni motion consists in a flow of the fluid ahead of the drop, resulting in the formation of a large wetting film behind, as shown in Figure 2 (top view). These films will be referred to as in situ created films. The specific interest of these in situ dewetting experiments is that both the coating and transfer steps into the bulk external liquid are eliminated, preventing thereby these systems from unwanted ex situ nucleation due to airborne contaminants (particles).

The second series of experiments are rather aimed to verify and support some basic hypotheses herein developed. In these

(18) Haidara, H.; Vonna, L.; Schultz, J. *J. Chem. Phys.* **1997**, *107*, 630.

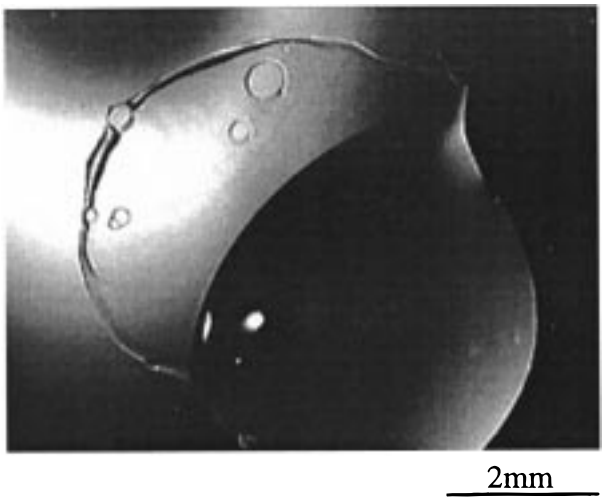

Figure 2. Top view of an in situ created liquid PDMS film showing a growing dewetting hole.

experiments, dewetting of pre-elaborated films (spin cast) onto HTS substrates is studied in both bulk pure water and homogeneous surfactant solutions (bulk concentration is cmc). The average thickness of these films, depending on the viscosity of the liquid PDMS, is in the micrometer range (~1 μm), as determined by ellipsometry. It is worthy of mention here that, for both in situ and ex situ dewetting experiments, the hole nucleation and growth take place spontaneously a few seconds after the film is immersed in the external fluid. No hole nucleation and growth is spontaneously observed in air for spin cast films during the transfer time or even over longer time scales (~0.5 h), as verified experimentally. This particular point which is related to the dewetting criterion of the metastable film, is presented and further discussed in the Appendix.

The use of *bulk* external liquids in these experiments is of primary importance regarding the reliability of the results. In fact, when very thin liquid layers are used as the external medium in these confined film dewetting experiments, extreme precautions should be taken to guarantee that this external liquid layer is omnipresent as a continuum phase and totally recovers the confined film. Otherwise, this external thin liquid layer may break or thin down from place to place, due to either evaporation (especially for volatile ones) or any other thickness fluctuation process (thermal, surface tension gradient, or airborne particles). In these cases, contrary to the present experiments, the results may be somewhat cautious because of the non-negligible probability for the confined film to dewet in air at some locations.

All the samples used in this work, the molecular self-assembled HTS surfaces and liquid PDMS films, have been elaborated through the same and quite reproducible processing path (cleaning, silanization, coating). In addition, fresh samples have been systematically used in each experiment to ensure reproducible results. The experimental observations were made using a video-recorder system. The images and data (hole size, kinetics, dewetting patterns, ...) were captured on a personal computer and analyzed using NIH image processing software.

Experimental Results: Raw Data

The first set of results concerns the dewetting behavior of in situ created liquid PDMS films by surfactant-induced Marangoni flow. A top view of this confined film showing a dewetting hole is given in Figure 2. The growing kinetics of the dewetting hole and the dependence of the dewetting velocity on the viscosity of the dewetting film, log V versus log η_{DL}, corresponding to these results are respectively plotted in parts a and b of Figure 3. Though no experimental mean has been used to check for the effective adsorption of the surfactant at the dewetting film−external liquid interface, the comparison of these in situ dewetting results with those obtained in bulk pure water

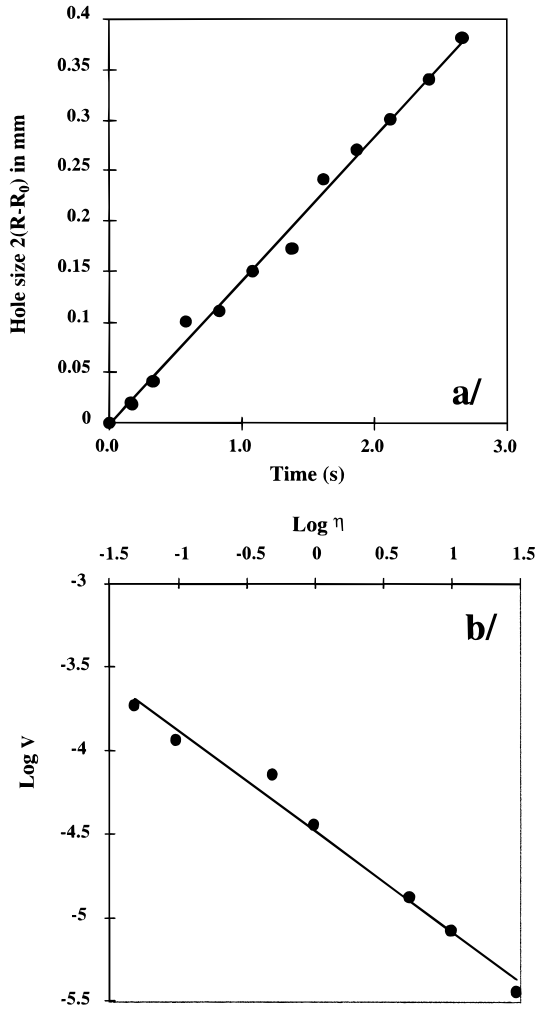

Figure 3. (a) Time dependence of hole growth $2(R(t) - R_0)$ for in situ created dewetting films: $R_0 = 32.5\ \mu$m; PDMS viscosity = 485 mPa·s. (b) Dewetting velocity as a function of PDMS viscosity, log V versus log η, for in situ created dewetting films.

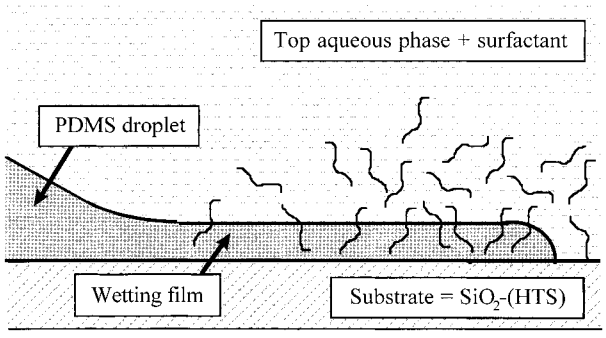

Figure 4. Structure and environment of the in situ created film.

and homogeneous surfactant solutions (see below) clearly indicates that a sufficient amount of surfactant may be present at this interface, as sketched out in Figure 4.

The second series of results is related to dewetting experiments involving the same liquid PDMS films which have been initially spin cast onto the substrate and then immersed in the external boundary liquid (pure water "W" and homogeneous surfactant solutions "SS"). For dewetting experiments in pure bulk water, these results are given as raw data in Table 1 for the characteristic parameters and dewetting velocities, and in parts a and b of Figure 5 for the hole-growing kinetics $R(t)$ and the

Table 1. Dewetting Data in Bulk Pure Water (W)[a]

PDMS oil viscosity η (mPa·s)	γ_{PDMS-W} (mJ·m^{-2})	θ_E (deg)	V_{PDMS} (μm·s^{-1})
9740	40	21 ± 1	0.6
4865	40	21 ± 1	0.6
971	40	21 ± 1	0.9
96	40	21 ± 1	1.7
9	40	18 ± 1	13

[a] Viscosity of water $\eta_W = 1$ mPa·s; $\gamma_{PDMS} = 20.5 \pm 0.5$ mJ m^{-2}.

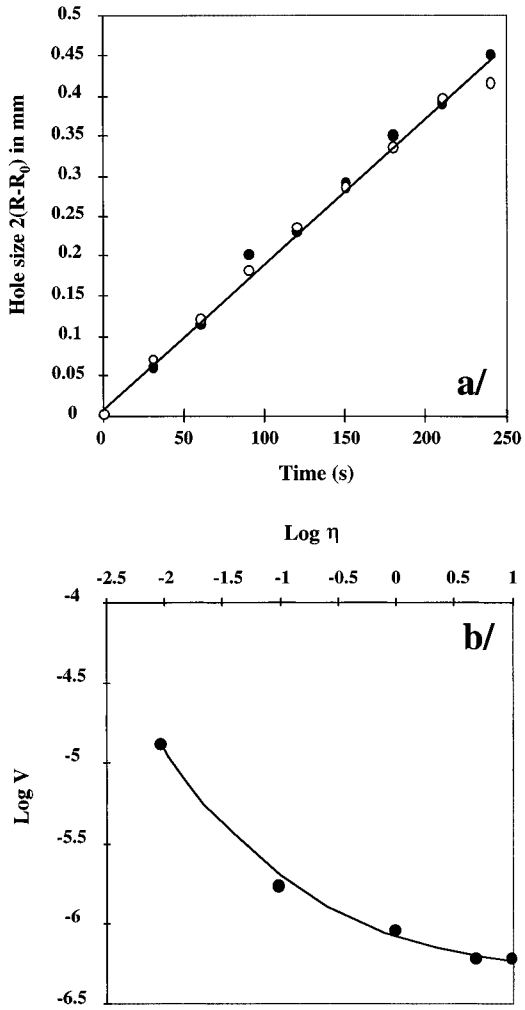

Figure 5. (a) Time dependence of hole growth $2(R(t) - R_0)$ for the dewetting in bulk pure water (W): data for two different holes (●, ○); (●) $R_0 = 30\ \mu$m; (○) $R_0 = 37.5\ \mu$m; PDMS viscosity = 971 mPa·s. (b) Dewetting velocity as a function of PDMS viscosity, log V versus log η, for the dewetting in bulk pure water (W).

Table 2. Dewetting Data in Homogeneous Surfactant Solutions (SS) at Bulk Concentration C = cmc and Viscosity $\eta_{SS} \sim \eta_W = 1$ mPa·s[a]

PDMS oil viscosity η (mPa·s)	$\gamma_{PDMS-SS}$ (mJ·m^{-2})	θ_E (deg)	V_{PDMS} (μm·s^{-1})
9740	10	46 ± 1	6.8
4865	10	46 ± 1	5.9
971	10	46 ± 1	17.5
96	10	46 ± 1	67.8
9	10	46 ± 1	340

[a] The surfactant is a trisiloxane−ethylene oxide compound.

viscosity dependence of the dewetting velocity $V(\eta)$, respectively. Similarly, Table 2 represents the raw data for the characteristic parameters and dewetting velocities in the bulk homogeneous surfactant solutions, while parts

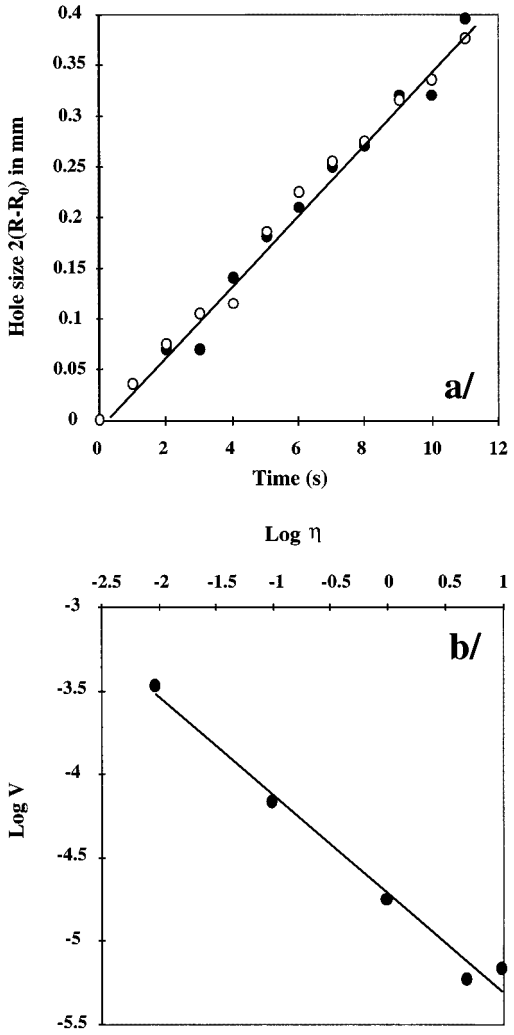

Figure 6. (a) Time dependence of hole growth $2(R(t) - R_0)$ for dewetting in bulk homogeneous surfactant solutions (SS): data for two different holes (●, ○); (●) $R_0 = 60\ \mu$m; (○) $R_0 = 42.5\ \mu$m; PDMS viscosity = 971 mPa·s. (b) Dewetting velocity as a function of PDMS viscosity, log V versus log η, for dewetting in bulk homogeneous surfactant solutions (SS).

a and b of Figure 6 represent respectively the hole-growing kinetics $R(t)$ and the viscosity dependence of the dewetting velocity $V(\eta)$. A typical dewetting pattern showing the growing holes in the homogeneous surfactant solutions is given in Figure 7 for a liquid PDMS film of viscosity $\eta = 970$ mPa·s.

These experimental results are discussed below, on the basis of both existing theoretical works and the specific nature of our systems where the presence of the surfactants may create some singularities and deviations from the theoretical predictions which mainly deal with pure fluids.

Discussion and Interpretation

Dewetting Experiments in Bulk Pure Water. These experiments belong to the dewetting regime $\theta_E < 1 << \eta_{DL}/\eta_{EL}$ and are characterized by a negligible Reynolds number associated with the flow in the bulk external phase (water), $R_e = \rho_W V h/\eta_w \sim 10^{-4}$. No viscoinertial effect is therefore expected in these experiments. Because all these basic assumptions are met for the dewetting of the liquid PDMS confined in the bulk pure water, the dewetting dynamics, especially the dependence of the velocity on the PDMS viscosity

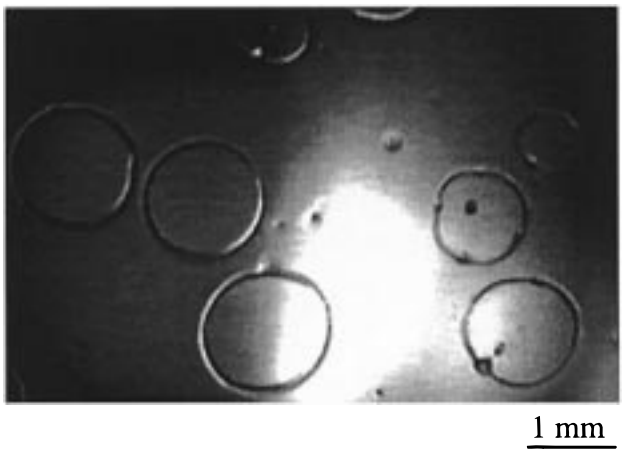

Figure 7. Top view of a dewetting film with growing holes in bulk surfactant solutions; the viscosity of the confined liquid PDMS is ~970 mPa·s.

$V_W(\eta_{PDMS})$, is expected to scale as $(\eta_{PDMS})^{-1}$ according to eq 5. As shown in Figure 5b, the plot of our raw experimental results seems to indicate *an apparent* deviation from expected $(\eta_{PDMS})^{-1}$ behavior, leading to a rather complex dependence $V \sim K_\eta(\eta_{PDMS})^{-\alpha}$, with $\alpha \neq 1$. It was then attractive in interpreting that *apparent* disagreement for the HTS−PDMS−W system to focus on the weak, though real dependence of the prefactor K_{DL} on the local molecular distribution and conformation within and around the moving edges of the rim. Some experimental evidence of such a dependence has already been established[13] in dewetting experiments involving metastable liquid PDMS films of different viscosities (from 95 up to ~60 000 mPa·s) at a hydrophobic solid−air interface. In these experiments, it was found that the series of PDMS with viscosities between 95 and 50 000 mPa·s was characterized by a unique numerical prefactor K_{DL}, as it appears in the expression of the dewetting in eq 5. In addition, this numerical prefactor happens to be significantly different from that characterizing higher viscosity liquid PDMS films. Since the liquid PDMSs used in our experiments have viscosities ranging mainly from 100 to 10000 mPa·s (Tables 1 and 2), the relevant question is then why this characteristic prefactor determined in air for that series is modified and split over in a water environment, leading to the apparent deviation from the expected $(\eta_{PDMS})^{-1}$ dependence. A partial answer at least to that question is given in Figure 8, which represents the adimensional plot of (V/V^*) against $(\theta_E)^3$, where $V^* = (\gamma_{PDMS-W}/\eta_{PDMS})$. As can be seen from this plot, a common value of $K_{DL}(\eta)$ given by the common slope is observed only for the three liquid PDMSs of lower viscosity. For higher viscosities a discrete and increasing $K_{DL}(\eta)$ value is found characterizing the behavior of each confined liquid PDMS film. Therefore, when plotting directly the raw experimental data, log V versus log η, no unique numerical prefactor characterizing the dewetting dynamics of this PDMS series in bulk external water can be found, contrary to their dewetting behavior in air. On the basis of this dependence of the numerical prefactor on both the viscosity of the dewetting film and the nature of the boundary phase, reduced dewetting velocities (V/K) rather than V have been considered and plotted against η, as shown in Figure 9. And as expected, we recover the predicted scaling behavior $(V/K)_{WATER} \sim (\eta_{PDMS})^{-1}$. The outstanding conclusion of these results regarding the scaling law $V(\eta)$ seems to be the strong dependence of the local structure and molecular parameters in the wedge on the nature of the external liquid (EL). This influence of the boundary liquid

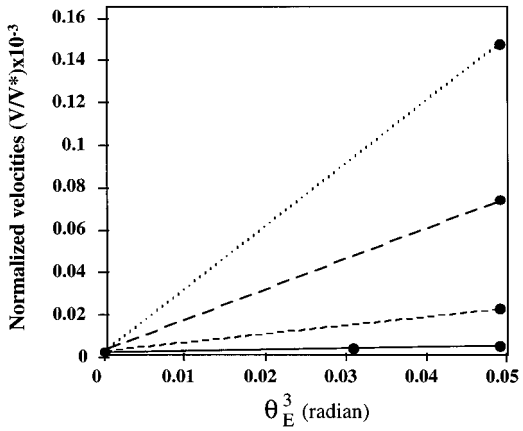

Figure 8. Viscosity dependence of the logarithmic prefactor for dewetting experiments in the external water medium. the prefactor is given by the slopes from the origin of (V/V^*) versus θ_E^3, where $V^* = (\gamma_{PDMS-W}/\eta_{PDMS})$.

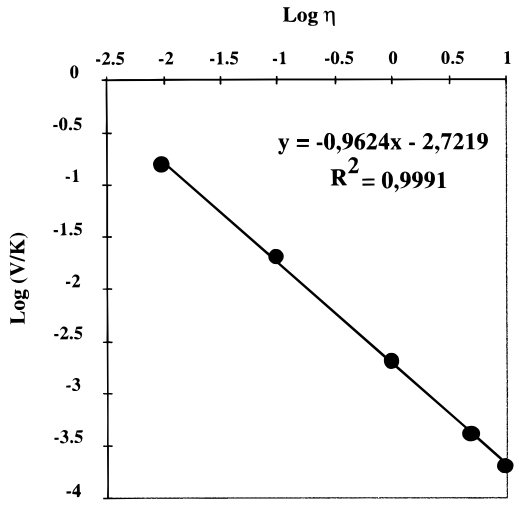

Figure 9. Reduced dewetting velocity as a function of the PDMS viscosity for dewetting experiments in bulk pure water; the velocity is reduced with respect to the viscosity-dependent prefactor $K = (12 \ln(h/a)\sqrt{2})^{-1}$: log (V/K) versus log η.

can either manifest through long-range forces (mainly van der Waals here), which are effective over the wedge scale especially when $\theta_D << 1$, or through phenomena such as partial miscibility, which may be enhanced by specific short-range interactions such as hydrogen or acid−base bonds between water molecules and siloxane segments (H−OH···O−Si−O). In support of these mechanisms one can refer to interfacial tension values currently measured for the liquid PDMS−W interface,[19−21] $\gamma_{PDMS-W} = 40 \pm 0.5$ mJ m^{-2}, which is about 20% less than what is expected from the relation[22]

$$\gamma_{PDMS-W} = \gamma_{PDMS} + \gamma_W - 2\sqrt{\gamma_W^{LW}\gamma_{PDMS}} = 50 \text{ mJ m}^{-2}$$

assuming as usual that methyl-terminated silicone oils are nonpolar liquids. On the other hand, for alkanes (C_n) which are effective van der Waals liquids, both measured

(19) Bergeron, V.; Langevin, D. *Macromolecules* **1996**, *29*, 306.
(20) Kanellopoulos, A. G.; Owen, M. J. *J. Colloid Interface Sci.* **1971**, *35*, 120.
(21) We confirmed this average value of PDMS−water interfacial tension given by other authors by tensiometry measurements where we get 40.5 mJ m^{-2}.
(22) Israelachvili, J. N. *Intermolecular and Surface Forces*, 2nd ed.; Academic Press: San Diego, CA, 1992.

and calculated γ_{Cn-W} values coincide[22] ($\simeq$50 mJ m^{-2}). The large discrepancy observed for liquid PDMS results mainly from the short-range hydrogen bond interactions which minimize γ_{PDMS-W} far beyond the value expected from purely dispersive interfacial forces. And this minimization of the interfacial tension may even result in the formation of a deeper interphase,[23] depending on both the temperature and solvating. As compared to dewetting experiments in air, these specific effects arising from the influence of the EL can alter both the structure and molecular parameters within the moving wedge: local viscosity (η), chain conformation (R_g), and density distribution (ρ) of the dewetting liquid. Therefore, when passing from the air environment to an active boundary phase, or from one EL to another, the logarithmic prefactor can no longer be considered as an intrinsic quantity characterizing the dewetting fluid but also as a function of the boundary phase $K(\eta,\text{DL}-\text{EL})$. For a given substrate and dewetting film, the magnitude, molecular weight, and viscosity dependence of this prefactor may be strongly altered from one external medium to another. Accordingly, the prediction that confined solid−liquid1−liquid2 systems satisfying the criterion $\theta_D < 1 << (\eta_{DL}/\eta_{EL})$ should dewet as solid−liquid1−air ones may involve this environment-dependent alteration of the logarithmic prefactor and consider the reduced velocities (V/K), rather than V. Though argued from fundamental considerations, an explicit formulation relating the dewetting dynamics to these alterations of the interfacial molecular features and wedge structure showing up in the prefactor $K(\eta,\text{DL}-\text{EL}) \sim (\ln(h/a))^{-1}$ may involve further theoretical consideration. Nevertheless, these results clearly show that the values of $K(\eta,\text{DL}-\text{EL})$ obtained in Figure 9 gradually increase from lower to higher molecular weights of the dewetting liquid, as already observed for liquid alkanes and PDMS in air.[13] This of course supports and stresses a strong dependence of the numerical prefactor on the nature of the external medium which can profoundly modify through the interface (forces, solvating, miscibility) the molecular size and conformation over the moving wedge.

Dewetting Experiments in Bulk Surfactant Solutions (SS). As for HTS−PDMS−W systems, dewetting experiments on pre-elaborated liquid PDMS films in external bulk homogeneous surfactant solutions (SS) involve the same range of viscosity (from 10 to 10 000 mPa·s). As shown in Table 2, which represents the characteristic parameters for these systems, contact angles and viscosity ratios are such that $\theta_D < 1 << (\eta_{PDMS}/\eta_{SS}$, where $\theta_D = \theta_E/\sqrt{2}$ with $\theta_E \sim 0.8$ and $\eta_{SS} \sim \eta_W \sim 1$ mPa·s for the homogeneous SS at bulk concentrations = cmc. Therefore, they belong as for dewetting experiments in pure water to the same theoretical regime where dewetting is expected to behave as at the PDMS−air interface, with a velocity scaling as $(\eta_{PDMS})^{-1}$. Here again, this prediction seems a priori violated for both dewetting experiments of pre-elaborated and in situ created liquid PDMS films in surfactant solutions. In addition, both these dewetting experiments in surfactant solutions result in the same scaling dependence of the dewetting velocity on η_{PDMS}, $V \sim (K\gamma)_{PDMS}(\eta_{PDMS})^{-0.6}$, as shown respectively in Figure 3b for the in situ created films and in Figure 6b for the pre-elaborated ones. As compared to the case of the external water medium, not only the scaling behavior $V(\eta)$ is modified in the aqueous surfactant solutions but also the magnitude of V:

(i) The dewetting velocity in surfactant solutions V_{SS} is about two orders higher than V_W in water (see Tables 1 and 2), whereas the opposite was expected on the basis of the drastic drop in the interfacial tension at the PDMS−SS interface, $\gamma_{PDMS-SS} \sim 1$ mJ m^{-2} at the cmc.

(ii) The viscosity dependence of the dewetting velocity $V_{SS} \sim (\eta_{PDMS})^{-0.6}$ differs from those observed in water, $(V_W/K_\eta) \sim (\eta_{PDMS})^{-1}$, or predicted from theories, $(\eta_{PDMS})^{-1}$, on the basis of the criterion $\theta_D < 1 << (\eta_{DL}/\eta_{EL})$.

Because of the higher dewetting velocity V_{SS} observed in the surfactant solutions, one could expect a crossover from the dewetting regime defined by $\theta_D < 1 << (\eta_{DL}/\eta_{EL})$ toward a viscoinertial regime where hydrodynamic flows induced in the surrounding fluid can account for the specific scaling law $V_{SS} \sim (\eta_{PDMS})^{-0.6}$. Such crossover from a viscous to viscoinertial regime is characterized[10] as discussed in previous sections by the Reynolds numbers of the flows $R_e = (\rho_{EL} V h/\eta_{EL}) > 1$. An estimate of this number for the dewetting experiments in the surfactant solutions leads to $R_e(\text{SS}) < 10^{-1}$, making unrelevant that viscoinertial dissipative regime in the external bulk phase. It then seems again from these results that the specific molecular and interfacial phenomena involved at the moving edges of the dewetting liquid film/external boundary fluid are predominant and definitely govern the dewetting dynamics.

In the following, we will try to show how further considerations of these local molecular features in the wedge, in relation to the overall numerical prefactor $K_{DL} = (12 \ln(h/a)\sqrt{2})^{-1}$, can bring some insights on these specific behaviors.

(i) Let us first assume that the numerical prefactors K_{DL} characterizing the dewetting in W and SS are comparable and relate the observed difference in the magnitude of the dewetting velocities to that of the unique contact angles. The maximum expected velocity ratio (V_{SS}/V_W) can then be estimated as follows.

For the SS where θ_E is quite close to 1 ($\sim$0.8), we will rather consider the actual values of $\cos\theta$ and $\tan\theta$ instead of the small angle ($\theta << 1$) expansions. Starting from eq 3 where the approximation $\theta_D = \theta_E/\sqrt{2}$ is no longer used, this leads for the SS to

$$V_{SS} \propto \left(\frac{\gamma_{PDMS-SS}}{\alpha_{SS}\eta_{SS}\tan\theta_D + (\eta \ln(h/a))_{PDMS}}\right)(\cos\theta_D - \cos\theta_E)\tan\theta_D \quad (6a)$$

For the external (W) medium where $\theta_E \sim 0.4 << 1$, eq 3 remains relevant and is specified as

$$V_W \propto \left(\frac{\gamma_{PDMS-W}}{\alpha_W\theta_E\eta_W + (\eta \ln(h/a))_{PDMS}}\right)\theta_E^3 \quad (6b)$$

Observing that $\alpha_W\theta_E$ (respectively $\alpha_{SS}\tan\theta_E$) $<< (\eta_{PDMS}/\eta_W)$, and upon eliminating the logarithmic factors assumed identical for both W and SS environments, the velocity ratio is obtained as

$$\frac{V_{SS}}{V_W} = \left(\frac{\gamma_{PDMS-SS}(\cos\theta_D^{SS} - \cos\theta_E^{SS})\tan\theta_D^{SS}}{\gamma_{PDMS-W}\theta(w)_E^3}\right) \quad (7a)$$

The interfacial tensions γ_{PDMS-W} and $\gamma_{PDMS-SS}$ are respectively 40 and $\sim$10 mJ·m^{-2} (at cmc). This latter value of the liquid PDMS/SS interfacial tension corresponds to the experimental value we measured by tensiometry upon 15 h of stabilization. One then can reasonably expect such an order of magnitude for $\gamma_{PDMS-SS}$ during the actual

(23) Chun, Y.; Li, D. *Colloid Surf., A: Physicochem. Eng. Aspects* **1996**, *113*, 51.

dewetting experiments where the interface may not be at equilibrium with respect to surfactant adsorption. Then, using the value $\gamma_{PDMS-SS} = 10$ mJ·m^{-2} in eq 7a where $\theta_E^3(W) = 0.06$, $\cos\theta_E(SS) = 0.7$ and $\gamma_{PDMS-W} = 40$ mJ·m^{-2} are determined from Tables 1 and 2, one obtains an estimate of the velocity ratio as $(V_{SS}/V_W) \cong 4(\cos\theta_D^{SS} - 0.7)\tan\theta_D^{SS}$. Therefore, for the ratio (V_{SS}/V_W) to be higher than 1, one needs the term $(\cos\theta_D^{SS} - 0.7)\tan\theta_D^{SS}$ to be greater than 0.25. This first implies the two terms $(\cos\theta_D^{SS} - 0.7)$ and $\tan\theta_D^{SS}$ must be simultaneously of identical sign for the product to be >0, regardless of its absolute value as compared to 0.25. For the relevant case under consideration where θ_D may reasonably be expected to lie between 0 and $\theta_E = 45°$ (~0.8 rad), for obvious physical reasons, we should allow θ_D to be finite, i.e. $\cos\theta_D < 1$; otherwise, no dewetting would have been observed. Actually, one expects from both current and previous works[24] θ_D to lie between the equilibrium contact angle in pure water $\theta_E(W) \sim 21°$ and that in the surfactant solution, $\theta_E(SS) \sim 45°$, for a bulk concentration = cmc. As one can see from simple calculations, the ultimate condition $(\cos\theta_D^{SS} - 0.7)\tan\theta_D^{SS} > 0.25$ necessary for V_{SS} to be higher than V_W can never be achieved, the maximum value of $(\cos\theta_D^{SS} - 0.7)\tan\theta_D^{SS}$ within the interval 0−45° being on the order of 10^{-1} for $\theta_D \sim 28°$. Therefore, the above hypotheses based on the sole consideration of the dewetting contact angles and interfacial tension values as adjustable parameters cannot account for the observed experimental result, $V_{SS} >> V_W$.

It then seems realistic to consider the possible variation of other physical parameters, especially the logarithmic prefactor entering the expression of V as given in eqs 6a and 6b. In the case where both contact angles and logarithmic factors are considered to be adjustable, the corresponding velocity ratio is simply obtained from eq 7a by incorporating the logarithmic terms as

$$\frac{V_{SS}}{V_W} = \left(\frac{\gamma_{PDMS-SS}(\cos\theta_D^{SS} - \cos\theta_E^{SS})\tan\theta_D^{SS}}{\gamma_{PDMS-W}\theta(w)_E^3}\right)\left(\frac{k_W}{k_{SS}}\right) \quad (7b)$$

where k_W and k_{SS}, respectively, stand for the $\ln(h/a)$ terms in water and surfactant solutions media, as given in eqs 6a and 6b.

Using the same numerical values for γ_{PDMS-W}, $\gamma_{PDMS-SS}$, and θ_E as before, the condition for the velocity ratio (V_{SS}/V_W) to be greater than 1 then follows as $(\cos\theta_D^{SS} - 0.7)\tan\theta_D^{SS} > 0.25(k_{SS}/k_W)$. We already know from the above discussion that the maximum value of $(\cos\theta_D^{SS} - 0.7)\tan\theta_D^{SS}$ is about 10^{-1} over the interval 0−45°. For the inequality $(\cos\theta_D^{SS} - 0.7)\tan\theta_D^{SS} > 0.25\ (k_{SS}/k_W)$ to be satisfied, one then needs the positive ratio (k_{SS}/k_W) be at least about the same order as the numerical factor 0.25, that is, $k_{SS}/k_W \sim 10^{-1}$. Taking this value as an estimate, the ultimate condition becomes $(\cos\theta_D^{SS} - 0.7)\tan\theta_D^{SS} > 0.025$. This condition is completely satisfied for any dynamic dewetting contact angle θ_D lying in the interval 5−40°, leading to an optimum velocity ratio $V_{SS}/V_W \sim 4$, for $\theta_D(SS) \sim 28°$. Amazingly these hypotheses not only satisfy the tendency observed experimentally, that is, $V_{SS} > V_W$, but they also result in a dewetting contact angle (~28°) which is quite close to what is expected (see eqs 3 and 4; theoretical section) from the assumption $\theta_D^{SS} = \theta_E^{SS}/\sqrt{2} \sim 32°$, where $\theta_E(SS) = 45°$ as mentioned above. If one now simultaneously assumes that the interfacial tension may be higher in the actual dynamic experiment where the interface is far from equilibrium and considers logarithmic factors $k_{SS}/k_W < 10^{-1}$, the relative magnitude observed experimentally for the dewetting velocities, $V_{SS}/V_W \sim 50$, is easily attained.

We should now seek physical arguments supporting the basic fact that the logarithmic prefactor $k \sim \ln(h/a)$ characterizing the dewetting dynamics of the same confined liquid PDMS can differ by orders of magnitude, depending on the boundary environment involved. As we already discussed above for the dewetting experiments in pure water, a mechanism which may support this fact is the alteration of the molecular features within the moving wedge due to interfacial forces and local miscibility, and which shows up in both the logarithmic cutoff a and the rim size h. In addition, a dissipative contribution from Marangoni flows, induced by the surfactant concentration gradient over the moving rim−solution interface[10,25,26] may be expected for dewetting experiments in surfactant solutions (see Chapter VII, paragragh 63 for ref 25). For viscous interfaces where finite relaxation times are required for the surfactant distribution to be uniform (grad $\Gamma \rightarrow 0$) over the interface, the boundary conditions are modified to include the resulting tangential stress, $\tau = \eta_{DL}(V/h) = (\partial\gamma/\partial\Gamma)\nabla\Gamma \sim \partial\gamma/\partial x$, regardless of the respective magnitude of θ_D and η_{DL}/η_{EL}. This arises at the DL/EL boundary in an average tangential force $F_T \sim (\gamma^R - \gamma^A)_{DL-EL}$, where γ^R and γ^A refer to interfacial tensions at receding and advancing sides of the moving rim. Assuming such a surfactant-induced gradient to exist, the corresponding dissipation can be estimated by considering the new force balance involving the above tangential force F_T, the previous friction forces F_V (eqs 2b and 2d) at external−dewetting liquid and solid−dewetting liquid interfaces, and the capillary driving force F_D (eq 1). Taking into account only the main dissipation from the solid−liquid interface and the new contribution from the interfacial tension gradient, the total viscous force F_V^* is obtained as[27] $F_V^* = (k_{DL}/\theta_D)\eta_{DL}V - (\gamma^R - \gamma^A)/2$. The capillary driving force F_D^* is now written as $F_D^* \propto \gamma^A(\theta_E^2 - \theta_D^2) + \gamma^R\theta_D^2 = (\gamma^R - \gamma^A)\theta_D^2 + \gamma^A\theta_E^2$, where one has used the fact that the equilibrium contact angle of the advancing side of the liquid rim is zero on the native liquid film. Upon equating these two terms, one ends with the following expression for the dewetting velocity in surfactant solutions, $V_{SS} = ((\gamma^R = \gamma^A)(\theta_D + \theta_D^3) + \gamma^A\theta_E^3)/k\eta$. As compared to eq 5, this does not modify the scaling behavior of V and constitutes a very negligible correction of magnitude to account for the observed difference, $V_{SS} \sim (10-10^2)V_W$. Again, these results and discussions seem to support the hypothesis of alteration of the logarithmic prefactor and its viscosity dependence. The magnitude of this alteration depends on the nature of the surrounding external medium and the specific interfacial phenomena it can induce at the interface. The local structure of the moving wedge is then affected through the dependence of the logarithmic prefactor on the molecular conformation, distribution, and composition (R_g, ρ, η) in its neighborhood, as discussed recently by E. Ruckenstein.[26] Incidentally, such an influence of the wedge structure on the cutoff length has already been discussed by de Gennes for the

(24) Haidara, H.; Vonna, L.; Schultz, J. *Langmuir* **1996**, *12*, 3351.

(25) Landau, L. D.; Lifshitz. E. M. *Fluid Mechanics*, 2nd ed.; Course of Theoretical Physics Vol. 6; Pergamon Press: New York, 1987.

(26) Ruckenstein. E. *J. Colloid Interface Sci.* **1996**, *179*, 136.

(27) de Gennes, P. G. In *Liquids at Interfaces*, *Les Houches*; Charvolin, J., Joanny, J. F., Zinn-Justin, J., Eds.; North-Holland: Amsterdam, 1988.

spreading of a droplet over a wet surface.[28] In the macroscopic regime where the thickness of the initial liquid film e_0 is >100 nm, a larger logarithmic cutoff a scaling as (e_0/θ_D) was expected, which corresponds to a smaller logarithmic prefactor $k \sim \ln(h/a)$ and should lead to an equally higher spreading velocity[28] (Part I, Section IV.C.4).

The influence of these interactions between the external and the dewetting liquids does not show up exclusively on the magnitude of the logarithmic prefactor $k_{DL} = \ln(h/a)$ but also involves its viscosity dependence $k_{DL}\{\eta_{DL}(EL)\}$, as revealed in the different scaling behaviors $V(\eta)$ observed for the two surrounding media (W and SS).

Finally, coming back to the dewetting velocity in SS, $V_{SS} \sim (\eta_{PDMS})^{-0.6}$, one can notice that in spite of the unfully explained scaling exponent, the plotted raw data log V_{SS} versus log η_{PDMS} all exhibit the same linear behavior for dewetting experiments involving surfactant solutions, as shown in Figures 3b and 6b, respectively, for in situ and pre-elaborated films. The main outcome of this result is that the whole PDMS series seems to be characterized by a unique prefactor in the dewetting experiments in surfactant media, as opposed to experiments in pure water, where the linear behavior was obtained only upon plotting the raw data in the reduced scale $\log(V_W/K)$ versus log η_{PDMS}, where $K_D = (12 \ln(h/a)\sqrt{2})^{-1}$. An interesting question arising from this specific and common scaling behavior $V_{SS} \sim (\eta_{PDMS})^{-0.6}$ observed for the two dewetting experiments in surfactant solutions is whether this behavior is characteristic of the dewetting dynamics of confined films involving complex media. Further investigations are needed before any serious answer can be made to this question.

Conclusion

Dewetting dynamics of confined metastable liquid PDMS films from a nonwettable substrate have been investigated in various boundary bulk liquids, pure water, and aqueous surfactant solutions. The magnitude and the scaling behavior of the dewetting velocity of the confined films were studied in these external environments and discussed through existing theoretical predictions. Apparent deviations from these predictions were observed, especially for dewetting experiments in external surfactant solutions. These deviations were discussed, on the basis of the assumed alteration of the logarithmic prefactor and wedge structure which are shown to depend strongly on the nature of the interacting external liquid.

The main outcome of this work is that one cannot just transpose the predicted scaling behaviors, $V(\eta)$ for instance, from one environment to another, because of that strong environment-dependent alteration experienced by the fluid within the moving wedge (molecular conformation, distribution, composition, local viscosity, ...). And this alteration of the local physical properties definitely shows up in both the magnitude and scaling behavior of the dewetting velocity $V(\eta)$, especially when complex media are involved, as was the case in this work for dewetting experiments in external surfactant solutions.

Appendix

As already mentioned in the Experimental Section, one returns in this Appendix to the hole nucleation and growth conditions which led us during these studies to some interesting observations. Though these nucleation steps do not constitute the main focus of this work, the relevance of these observations appears to deserve at least a few comments. The most important of these observations is that no hole nucleation and growth was observed in air for the pre-elaborated films (~1 μm spin cast), during the time involved in their preparation and transfer into the bulk external liquid (~30 s). This stability of the metastable films in air was verified over an even longer time scale, up to 0.5 h. On the other hand, the nucleation−growth process starts quite spontaneously upon their immersion in both aqueous phases (~5 s), the shortest nucleation−growth time being observed for the surfactant solutions. *These observations rather account for the probability of spontaneous hole nucleation and growth in confined films of identical thickness in different environments, both confined system being characterized by a negative spreading parameter* $S_{I/S} = \gamma_{SJ} - \gamma_{SI} - \gamma_{IJ} = \gamma_{IJ}(\cos\theta - 1)$. Using experimental data already given in this paper, these spreading parameters are respectively $S_{AIR} \approx -0.5$ mJ·m^{-2}, $S_W \approx -2.5$ mJ·m^{-2}, and $S_{SS} \approx -3$ mJ·m^{-2} (for $\gamma_{PDMS-SS} = 10$ mJ m^{-2}) or -0.3 mJ·m^{-2} (for $\gamma_{PDMS-SS} = 1$ mJ·m^{-2}). In the limit of microsize[13,29] dewetting films considered here, and so long as comparative dewetting behaviors are considered, gravity effects can be neglected. In the following, a simple formulation of the spontaneous dewetting probability (time life before nucleation−growth) of the metastable HTS−liquid PDMS film in the different environments (air versus bulk liquids) is proposed, on the basis of simple surface energetic considerations.

Let us first calculate the interfacial free energy associated with the nucleus, F_{NUCL}, as represented in Figure 1, where the area involved is given by $A_{NUCL} = \pi^2 Rh + \pi R^2$. The first term corresponds to the generated rim surface (half cylinder), and the second corresponds to the solid−EL interface. The corresponding interfacial free energy of the nucleus is then

$$F_{NUCL} = \pi^2 Rh\gamma_{DL-EL} + \pi R^2\gamma_{S-EL} \qquad \text{(A1)}$$

Comparing this to the free energy corresponding to the initial flat interface configuration

$$F_{FLAT} = \pi R^2(\gamma_{S-DL} + \gamma_{DL-EL}) \qquad \text{(A2)}$$

where the area involved is πR^2 on both sides of the thin (DL) disk, one gets the interfacial free energy variation due to the nucleation process as

$$\Delta F_{NUCL} = \pi R^2(\gamma_{S-EL} - \gamma_{DL-EL} - \gamma_{S-DL}) + \pi^2 Rh\gamma_{DL-EL} \qquad \text{(A3)}$$

or equivalently

$$\Delta F_{NUCL} = \pi R^2 S_{(DL/S)EL} + \pi^2 Rh\gamma_{DL-EL} \qquad \text{(A4)}$$

(i) Because ΔF_{NUCL} should be <0 for the nucleus to grow as a dewetting hole, relation A4 just tells that this will never happen so long as $S_{(DL/S)EL}$ is ≥0, since γ_{DL-EL} is always ≥0. This is already a well-known result.

(ii) The second situation which is of more concern for our discussion is that of a metastable solid−dewetting liquid−external liquid system, with $S_{(DL/S)EL} < 0$. One then expects in this case ΔF_{NUCL} to be <0 under some conditions, leading to spontaneous dewetting over a characteristic time scale which, for a given solid−dewetting film, depends essentially on the external boundary phase. Putting back into eq A4 these conditions, $S_{(DL/S)EL}$

(28) de Gennes, P. G. *Rev. Mod. Phys.* **1985**, *57*, 827.

(29) Sharma, A.; Ruckenstein, E. *J. Colloid Interface Sci.* **1989**, *133*, 358.

< 0 and $\Delta F_{NUCL} < 0$, one gets

$$\pi R^2 |S_{(DL/S)EL}| > \pi^2 R h \gamma_{DL-EL} \quad \text{(A5)}$$

Equation A5 can be written in a more condensed form, using a critical nucleation parameter $\lambda_C = (R_C/h_C)$ to be reached before dewetting can set in, as

$$\left(\frac{R_{NUCL}}{h_{RIM}}\right) > \lambda_C = \pi\left(\frac{\gamma_{DL-EL}}{|S_{(DL/S)EL}|}\right) \quad \text{(A6)}$$

Equation A6 tells us that, beyond the spreading parameter $S_{(DL/S)EL} < 0$, the film will dewet by hole nucleation only when the characteristic parameter R_{NUCL}/h_{RIM} of the nuclei is larger than a critical nucleation parameter of the system, λ_C, given by the dimensionless capillary quantity $\lambda_C = \pi(\gamma_{DL-EL}/|S_{(DL/S)EL}|)$. Otherwise, the corresponding initial hole (nucleus) should heal and no dewetting will be observed. This simple energetic picture related to usual capillary parameters of the system finally leads to an equally simple and predictable nucleation-induced dewetting probability for a given confined metastable film of thickness t, depending on both boundary phases (solid and external). Incidentally, when one neglects the numerical prefactor π and makes use of the fact that the elastic modulus μ of the rubber phase just scales as $\mu \sim \gamma/e$, where γ and e are respectively the surface tension and the characteristic size of a layer under local deformations, criterion A6 is identical to that derived by Brochard-Wyart[2] for the expansion of dewetting holes in systems involving a rubber phase boundary.

When applied to the different dewetting systems discussed above, using the proper $\gamma_{PDMS-EL}$ and $S_{DL/EL}$ values, criterion A6 leads respectively to

$$(R/h)_{AIR} > \lambda_C \approx 130, \quad (R/h)_{WATER} > \lambda_C \approx 50, \quad \text{and}$$
$$(R/h)_{SURF.SOLUT} > \lambda_C \approx 10$$

These values clearly show why the probability of spontaneous nucleation and growth leading to dewetting is negligibly low in air for these HTS−PDMS films, even in the presence of microsize defects, making necessary the use of artifices to induce that nucleation and growth.

On the other hand, the fast nucleation and growth of dewetting holes for the same HTS−PDMS films immersed in external W or SS liquid is simply related to the much lower value required for the critical nucleation parameters λ_C for dewetting to set in, about an order smaller for the SS versus air. This criterion may also determine somehow, through the equal probability of hole creation over the film, both the hole density and final dewetting pattern, as we observed in recent experiments. Because it involves usual and accessible capillary parameters ($\gamma/|S|$), this criterion may constitute for current technological applications a simple means to select among different systems the best fluid formulation (coating) or surface treatment qualified for the required stability of the system throughout a processing "time window".

LA9709756